JACS JOURNAL OF THE AMERICAN CHEMICAL SOCIETY
pubs.acs.org/JACS
Article

Ketone Enolization with Sodium Hexamethyldisilazide: Solvent- and Substrate-Dependent *E*–*Z* Selectivity and Affiliated Mechanisms

Ryan A. Woltornist and David B. Collum*

Cite This: *J. Am. Chem. Soc.* 2021, 143, 17452–17464
Read Online

ACCESS | Metrics & More | Article Recommendations | Supporting Information

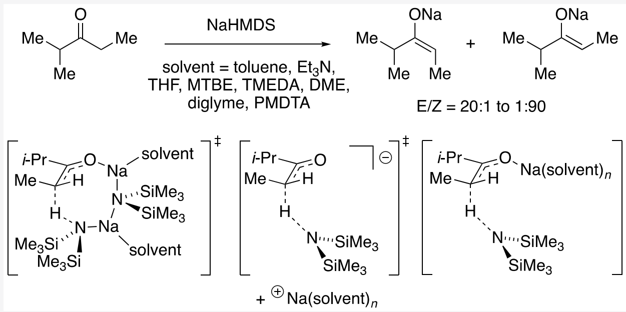

ABSTRACT: Ketone enolization by sodium hexamethyldisilazide (NaHMDS) shows a marked solvent and substrate dependence. Enolization of 2-methyl-3-pentanone reveals *E*–*Z* selectivities in Et_3N/toluene (20:1), methyl-*t*-butyl ether (MTBE, 10:1), *N,N,N′,N″,N″*-pentamethyldiethylenetriamine (PMDTA)/toluene (8:1), TMEDA/toluene (4:1), diglyme (1:1), DME (1:22), and tetrahydrofuran (THF) (1:90). Control experiments show slow or nonexistent stereochemical equilibration in all solvents except THF. Enolate trapping with Me_3SiCl/Et_3N requires warming to −40 °C whereas Me_3SiOTf reacts within seconds. In situ enolate trapping at −78 °C using preformed NaHMDS/Me_3SiCl mixtures is effective in Et_3N/toluene yet fails in THF by forming $(Me_3Si)_3N$. Rate studies show enolization via mono- and disolvated dimers in Et_3N/toluene, disolvated dimers in TMEDA, trisolvated monomers in THF/toluene, and free ions with PMDTA. Density functional theory computations explore the selectivities via the *E*- and *Z*-based transition structures. Failures of theory-experiment correlations of ionic fragments were considerable even when isodesmic comparisons could have canceled electron correlation errors. Swapping 2-methyl-3-pentanone with a close isostere, 2-methylcyclohexanone, causes a fundamental change in the mechanism to a trisolvated-monomer-based enolization in THF.

INTRODUCTION

We have become infatuated with the untapped potential of organosodium chemistry.[1] Over a century in which organolithium chemistry flourished, organosodium chemistry languished despite the prevalence and low cost of sodium.[2,3] It is difficult to find examples in which sodium-based reagents are used for sophisticated or nuanced applications in stereo- or regiocontrolled organic synthesis.[4] While it might be tempting for the mechanistically minded to attribute this to a dearth of underlying solution structural and mechanistic principles,[5−7] there is scant evidence that a lack of physical principles impedes the empiricism-based development of new methods. A perceived inconvenience of the obvious foundational reagents *n*-butylsodium (*n*-BuNa) and sodium diisopropylamide (NaDA), when compared with commercially available *n*-butyllithium (*n*-BuLi) and lithium diisopropylamide (LDA) could have stifled development, but even that impediment was probably exaggerated and is now largely resolved.[1,8]

The preeminent organosodium reagent that has *not* been ignored by the synthetic community is sodium hexamethyldisilazide (NaHMDS).[8−12] It is soluble, stable, and commercially available in toluene and tetrahydrofuran (THF). NaHMDS is used in both academic and industrial laboratories on micro-to-plant scales.[13,14] Nevertheless, whereas crystallographers have characterized a number of synthetically relevant NaHMDS solvates,[15] solution structural and even computational studies were nearly nonexistent.[16,17] Hoping to nudge researchers to consider a broader range of conditions, we determined the aggregation and solvation states of NaHMDS in over 30 mono-, di-, and polyfunctional solvents.[18] Emblematic solution structures **1**–**7** germane to the mechanistic studies described herein are shown in Chart 1.

We offer herein our first efforts to add a few mechanistic details—an intellectual basis set so-to-speak—to correlate

Chart 1. Select Solution Structures of NaHMDS

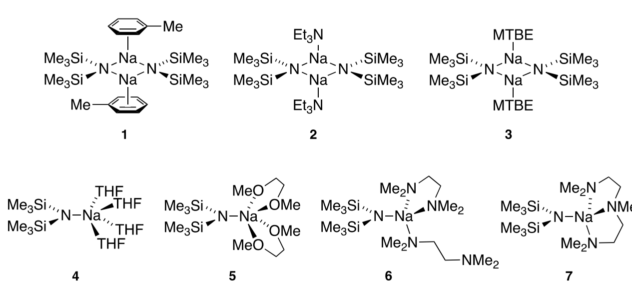

Received: June 23, 2021
Published: October 13, 2021

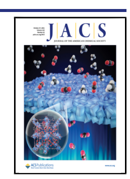

solution structures of NaHMDS with reactivities and selectivities using ketone enolizations as a template (eq 1).[19]

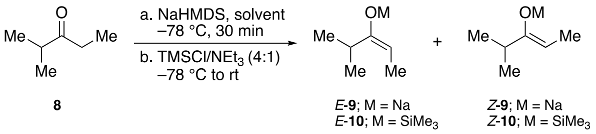

(1)

E/Z = 20:1 to 1:90

We got lucky in that unexpectedly high and highly solvent-dependent *E*−*Z* selectivities serve as benchmarks to correlate selectivity with the mechanism.[20] (Of the several hundred easily identified NaHMDS-derived *E*−*Z* selectivities, they *all* use THF.)

Although few would doubt that sodium-based reagents are much more reactive than their lithium analogs, we were not even confident predicting something so simple as the relative reactivities of NaHMDS versus LiHMDS let alone if the solvent-dependent reactivities of NaHMDS span a factor of 5 or 5 orders of magnitude.[19] The following relative reactivities toward enolization of ketone **8** reveal that such simple questions are insufficiently nuanced:

	$LiHMDS/Et_3N$ >	NaHMDS/THF >	$NaHMDS/Et_3N$ >	LiHMDS/THF
k_{rel}	160	55	2	1

Detailed rate studies using a small sampling of solvents revealed a bewildering array of dimer-, monomer-, ion pair-, and free ion-based mechanisms. By happenstance, we also discovered that isosteric ketones **8** and **11** (eq 2), despite relative rates in 4.0 M THF/toluene that are nearly identical ($k_{rel} \approx 1.0$), *enolize via fundamentally different mechanisms.*

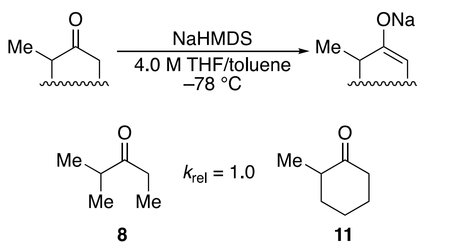

(2)

This first examination of the mechanistic underpinnings of NaHMDS reactivity has served up a wealth of surprises. To assist the reader, we separate counterintuitive arithmetic oddities relating to kinetics—there are quite a few—from the complexities of organosodium chemistry. The Background section begins with possible generic mechanisms and arithmetic subtleties within the rate laws.

■ BACKGROUND

A useful maxim is that rate laws provide the stoichiometries of rate-limiting transition structures relative to the reactants.[21] Complex mechanisms are merely composites of the separate contributions.[22,23] This section describes the graphical and arithmetic consequences of nine mechanisms, seven of which are implicated in the rate studies herein while two others are both plausible and pedagogically useful. We use a shorthand in which A = $(Me_3Si)_2N^-$ anion, Na = Na^+ cation, K = ketone, and S = solvent or ligand. (We use solvent and ligand interchangeably.) The shorthand is illustrated with the three generalized reactants of interest, **12**−**14**.

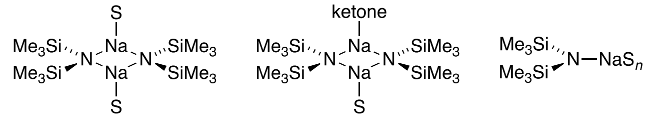

$A_2Na_2S_2$ **12** A_2Na_2SK **13** $ANaS_n$ **14**

A = $(SiMe_3)_2N^{\ominus}$; Na = $Na^{\oplus}$, S = solvent; K = ketone

Mechanism A. The simplest imaginable enolization starts from an observable monomer and proceeds via a monomer-based transition structure (eqs 3−5). The first-order dependencies in substrate and NaHMDS would be accompanied by a solvent order that could, in theory, span a range but would likely be zero (if no change in solvation is required) or inverse-first order (rate ∝ 1/[S]) if a sodium−substrate interaction requires a solvent dissociation.

Monomer to monomer:

$$ANaS_n \pm S \rightleftharpoons ANaS_{n\pm1} \quad (3)$$

$$ANaS_{n\pm1} + K \rightarrow \text{enolate} \quad (4)$$

$$-d[K]/dt \propto [ANaS_n]^1[K]^1[S]^{\pm1} \quad (5)$$

Mechanism B. Structural studies showed a penchant for NaHMDS to form ion pairs in strongly dipolar solvents. Rate studies suggest that ionizations to form fleeting ion pairs are facile for lesser solvents as well (eqs 6−8). Because the two ions are electrostatically correlated (bound), the ion pairs are kinetically indistinguishable from covalently bound monomers; both would display first-order dependencies in NaHMDS.[24,25] However, an ion pair-based mechanism would likely (although not necessarily) manifest a positive solvent order to fill the sodium ion coordination shell.

Monomer to ion pair:

$$ANaS_n + mS \rightleftharpoons A^{\ominus}//^{\oplus}NaS_{m+n} \quad (6)$$

$$A^{\ominus}//^{\oplus}NaS_{m+n} + K \rightarrow \text{enolate} \quad (7)$$

$$-d[K]/dt \propto [ANaS_n][K]^1[S]^m \quad (8)$$

Mechanism C. Free ion-based enolizations appeared unexpectedly (eqs 9−11). Free ions are distinguished from ion pairs in that the absence of electrostatic attraction causes them to function as independent fragments.[24]

Monomer to free ions:

$$ANaS_n + mS \rightleftharpoons A^{\ominus} + {}^{\oplus}NaS_{m+n} \quad (9)$$

$$A^{\ominus} + K \rightarrow \text{enolate} \quad (10)$$

$$-d[K]/dt \propto [ANaS_n]^{1/2}[K][S]^{m/2} \quad (11)$$

To obtain the rate law in eq 11, the equilibrium in eq 9 is described by eq 12. Equating the amide and sodium free ions (eq 13) and solving for the concentration of amide anion, $[A^-]$, affords eq 14, which shows the critical components of the rate law in eq 11. The algebra not only predicts a half-order dependence on the NaHMDS monomer but also introduces the possibility of fractional orders in the solvent term if the mechanism demands an *odd* number of additional solvents (m = 1 or 3).[24] The fractional orders in the NaHMDS monomer *and* free solvent are highly diagnostic.

https://doi.org/10.1021/jacs.1c06529
J. Am. Chem. Soc. 2021, 143, 17452−17464

$$K_{eq} = [A^{\ominus}][^{\oplus}NaS_{m+n}]/[ANaS_n][S]^m \quad (12)$$

$$[A^{\ominus}] = [^{\oplus}NaS_{m+n}] \quad (13)$$

$$[A^{\ominus}] = K_{eq}{}^{1/2}[ANaS_n]^{1/2}[S]^{m/2} \quad (14)$$

With the understanding of the arithmetic consequences established, we must note that a triple ion-based metalation[26] involving free ions (eq 15) would be kinetically indistinguishable from monomer- or ion pair-based mechanisms (Mechanisms A or B); the second-order contribution of associating two amido fragments is offset by the half-order dependence imposed by the free ionization.[24] We have invoked triple ions in the past but have insufficient evidence to invoke one in our current studies, recognizing that we could be in error. None of the enolizations manifest autoinhibition from the accumulation of the sodium ions because of the reassociation with the enolate fragment.

$$2ANaS_n \rightleftharpoons A_2Na^{\ominus} + {}^{\oplus}NaS_{2n} \quad (15)$$

There is an acutely unintuitive arithmetic oddity: single-solvent ligation to form an ion pair (Mechanism B) and double-solvent ligation to give a free ion would both manifest first-order solvent dependencies. The two mechanisms are distinguished by the NaHMDS orders.

Mechanism D. Dimeric NaHMDS dominates in poorly coordinating solvents.[18] As found previously in lithium amide chemistry, these weak solvents can promote dimer-based mechanisms,[23] the simplest of which is shown in eqs 16–18. First-order dependencies on NaHMDS dimer and ketone would be accompanied by solvent orders depending on whether the mechanism requires a fleeting solvent dissociation (rate ∝ 1/[S]), a disolvated dimer (zeroth-order), or additional solvation (a positive integer order). This dimer mechanism as drawn has not been observed for NaHMDS yet, but a close relative is described below.

Dimer to dimer:

$$A_2Na_2S_2 + nS \rightleftharpoons A_2Na_2S_{2+n} \quad (16)$$

$$A_2Na_2S_{2+n} + K \rightarrow \text{enolate} \quad (17)$$

$$-d[K]/dt \propto [A_2Na_2S_2][K][S]^n \quad (18)$$

Mechanism E. The dimer-based mechanism described by eqs 19 and 20 is distinguished from that in Mechanism D by the *observable* formation of a ketone-complexed dimer (**13**). It is a subtle distinction with some nontrivial influences on the rate behavior. The substrate is formally the NaHMDS–ketone complex **13** and would afford a first-order dependence on **13**, a *zeroth-order* dependence on free NaHMDS dimer, and a solvent order that reflects the number of added solvents ($n \geq 0$). The base concentration-independent rate for a base-mediated reaction is quirky at first blush but precedented[23] and highly diagnostic.

Complexed dimer to dimer:

$$A_2Na_2SK + nS \rightarrow \text{enolate} \quad (19)$$

$$-d[K]/dt \propto [A_2Na_2SK][A_2Na_2S_2]^0[S]^n \quad (20)$$

Mechanism F. If an observably complexed dimer (A_2NaSK) reacts via a monomer-based pathway (eqs 21–23), it would manifest an *inverse* half-order dependence on NaHMDS (rate ∝ $1/[A_2NaS_2]^{1/2}$). Such a counterintuitive inhibition of a base-mediated metalation *by the base* has been observed[23,27] but not in this study. It would be difficult to miss.

Complexed dimer to monomer:

$$A_2Na_2SK + nS \rightleftharpoons ANaS_nK + 1/2A_2Na_2S_2 \quad (21)$$

$$ANaS_nK \rightarrow \text{enolate} \quad (22)$$

$$-d[K]/dt \propto [A_2Na_2SK][A_2Na_2S_2]^{-1/2}[S]^n \quad (23)$$

Mechanism G. A mechanism in which amide dimers deaggregate to monomers (eqs 24–26) is by far the most prevalent seen in the chemistry of LDA and related lithium amides.[23] The characteristic half-order dependence is often accompanied by zeroth- or first-order solvent dependencies in the lithium amides. The corresponding ion pair-based mechanism would display the same NaHMDS order but would likely manifest an elevated solvent order, n, to attain a four- or higher-coordinate sodium cation.

Dimer to monomer:

$$1/2A_2Na_2S_2 + nS \rightleftharpoons ANaS_{1+n} \quad (24)$$

$$ANaS_{1+n} + K \rightarrow \text{enolate} \quad (25)$$

$$-d[K]/dt \propto [A_2Na_2S_2]^{1/2}[K][S]^n \quad (26)$$

Mechanism H. We would not have considered a free ion-based mechanism (eqs 27–29) in weakly coordinating solvents that afford an observable NaHMDS dimer had we not been schooled by the rate data. The standout property is a *one-fourth-order dependence* on the NaHMDS dimer. We have never observed an order even approximating one-fourth in lithium amide chemistry.[23] Although the one-fourth-order stems from the algebra, one can form a mental construct by imagining the superposition of dimer–monomer deaggregation (eq 24) and a monomer-free ion dissociation, each of which independently imposes half-order dependencies.[23,24] The square root embedded in the solvent order creates the potential for fractional solvent orders.

Dimer to free ion:

$$1/2A_2Na_2S_2 + nS \rightleftharpoons A^{\ominus} + {}^{\oplus}NaS_{1+n} \quad (27)$$

$$A^{\ominus} + K \rightarrow \text{enolate} \quad (28)$$

$$-d[K]/dt \propto [A_2Na_2S_n]^{1/4}[K][S]^{n/2} \quad (29)$$

Mechanism I. The last mechanism was foisted upon us during a control experiment (eqs 30–32). The association of two monomers to form a more reactive dimer is decidedly contrary to conventional wisdom, but the longstanding perceived correlation of high reactivity with lower aggregates has slowly eroded[28] as has the correlation of strong solvation with lower aggregates.[29]

Monomer to dimer:

$$2ANaS_n + mS \rightleftharpoons A_2Na_2S_{2n+m} \quad (30)$$

$$A_2Na_2S_{2n+m} + K \rightarrow \text{enolate} \quad (31)$$

$$-d[K]/dt \propto [ANaS_n]^2[K][S]^m \quad (32)$$

https://doi.org/10.1021/jacs.1c06529
J. Am. Chem. Soc. 2021, 143, 17452–17464

RESULTS AND DISCUSSION

General Methods. NaHMDS and [^{15}N]NaHMDS were prepared as white crystalline solids from hexamethyldizilazane and sodium metal.[18] There is no evidence the added precautions to purify NaHMDS for structural and mechanistic studies alter reactivity when compared with commercial samples. Owing to commercial availability being limited to toluene and THF, a preparation of NaHMDS in neat Et_3N in the Experimental Section illustrates the ease of synthesis in any donor solvent.

***E*−*Z* Selectivities.** Selectivities were monitored by enolizing ketone **8** under argon in standard vials fitted with septa. Samples were quenched with Me_3SiCl/Et_3N mixtures as described previously[30] and analyzed by gas chromatography. The two silyl ethers could also be distinguished by IR spectroscopy (vide infra). The solvent-dependent selectivities are summarized in Table 1. *E*-selective enolizations are highest for Et_3N/toluene whereas THF promotes exceptional *Z* selectivity. The probes of solvent- and solvent *concentration*-dependent selectivities were guided by both empiricism and the results from the mechanistic studies. For example, the selectivity drops to 8:1 for 1.5 M Et_3N/toluene owing to a competing less-selective pathway.

Table 1. *E*−*Z* Selectivities for the Enolization of Ketone 8-d_3 to Provide Enol Silyl Ethers *E*-10-d_2 and *Z*-10-d_2[a]

solvent	concentration (M)	*E*−*Z* ratio	k_{rel}
toluene	neat	6:1	1
Et_3N	4.00	20:1	6
MTBE	6.00	10:1	60
THF	9.00	1:90[b]	820
DME	2.00	1:20[c]	186
TMEDA	1.50	4:1	680
PMDTA	1.50	8:1	90
diglyme	2.00	1:1	

[a]0.10 M NaHMDS, 0.005 M ketone. Toluene, Et_3N, and MTBE were converted from rate constants determined using **8**-d_0 on the basis of a KIE of 12 ± 1, while all other rate constants were determined from the enolization of **8**-d_3. [b]Selectivity reflects full *E*−*Z* equilibration. [c]Selectivity reflects limited erosion of *E*−*Z* selectivity.

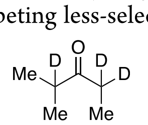

8-d_3

The rate and computational data suggest that kinetically controlled enolizations should generally show dominant *E* selectivity. Suspecting that reversible enolization (eq 33)

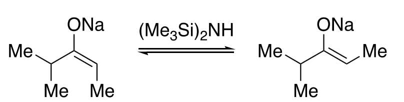

(33)

examined by Gaudemar and Bellassoued[31] was the source of the high *Z* selectivity in THF and possibly a source of stereochemical erosion in other solvents,[19a,32] we probed for equilibration by control experiments that became far more extensive than anticipated, as discussed below.

We replicated the reactions in Table 1 but with monitoring by IR spectroscopy. In the THF solution, the *E* and *Z* isomeric enolates *E*-**9** and *Z*-**9** appear as overlapping absorbances at 1610 and 1603 cm^{-1}, respectively,[33] and isomerize at rates comparable to the rate of enolization. Trapping with Me_3SiCl/Et_3N showed what the GC studies had suggested: the silylation half-life was approximately 20 m at −78 °C, which is far too slow to capture the kinetic *E*−*Z* selectivity. Switching to Me_3SiOTf without Et_3N elicited fast trapping ($t_{1/2}$ < 5 s), affording *E*-**10** (1689 cm^{-1}) and *Z*-**10** (1676 cm^{-1}). Prompt quenching of a NaHMDS/THF enolization **8** at completion (4.0 min) with Me_3SiOTf at −78 °C and GC analysis afforded a 1:4 *E*−*Z* selectivity. Although failing to fully capture the kinetic *E* selectivity, it confirms the rapid isomerization. Related studies with the other solvents in Table 1 showed limited erosion of only the NaHMDS/DME-mediated enolization.

Despite a focus on the chemistry of NaHMDS, not sodium enolates, we would be remiss to not mention a few oddities that emerged probing the isomerization. A number of controls showed that free ketone did *not* participate. Similarly, metalation of **8**-d_3 in the presence of excess $(Me_3Si)_2N$−H showed *no* (<2%) proton incorporation (eq 34). In short, simple proton

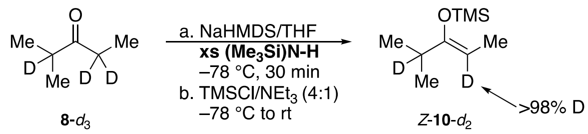

(34)

transfers were not implicated. Curiously, the metalation of **8** with NaHMDS/methyl-*t*-butyl ether (MTBE) or NaHMDS/Et_3N to generate the dominant *E*-**9** enolate, subsequent addition of THF, and aging at −78 °C for up to 60 min followed by silylation showed no equilibration whatsoever. We leave the reader with the current thoughts. Mounting evidence shows enolization at −78 °C affords *kinetically generated aggregates that are not equilibrated.*[34] Aggregate equilibrations can require warming to room temperature. An enolate *generated* in THF could be very different than an enolate generated in Et_3N or MTBE with *added* THF. As to *how* the *E*−*Z* isomerization takes place, we imagine a facile isomerization of O−Na and C−Na contacts of the ambident anion might be involved.

On a final note, during efforts to capture the kinetic selectivity prior to equilibration, we examined the use of preformed NaHMDS/Me_3SiCl mixtures for in situ trapping first exploited in the early 1980s.[35] As shown in Scheme 1, silylation of NaHMDS afforded exclusively $(Me_3Si)_3N$ in THF, but Et_3N/toluene mixtures afforded excellent conversion and 15:1 *E*−*Z* selectivity comparable to that in the stepwise protocol.

Scheme 1. Solvent-Dependent In Situ Trapping

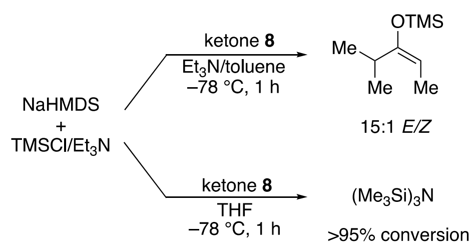

Rate and Computational Studies: General. Reaction rates were monitored using in situ IR spectroscopy[36] under pseudo-first-order conditions following the loss of ketone (1719 cm^{-1} for **8** and 1715 cm^{-1} **8**-d_3) as the limiting reagent and the formation of enolate *E*-**9**−*Z*-**9** (1599−1610 cm^{-1}). Complexation of the starting ketone to the NaHMDS dimer was detected by a shift in the carbonyl absorbance (**8** = 1712 cm^{-1}; **8**-d_3 = 1704 cm^{-1}) only in toluene, Et_3N/toluene, TMEDA/toluene,

https://doi.org/10.1021/jacs.1c06529
J. Am. Chem. Soc. 2021, 143, 17452−17464

and very low MTBE concentrations in MTBE/toluene. Similar perturbations in the carbonyl absorbances are documented for ketone−lithium amide complexes.[19,37,38] A monotonic 2 Hz rise in the ^{29}Si−^{15}N coupling constant resulting from incremental additions of ketone **8** to [^{15}N]NaHMDS/Et_3N/toluene affirmed the complexation.[18] Enolization rates at −78 °C were modulated for maximal convenience using **8** and its deuterated analog (**8**-d_3).[39] All enolizations display kinetic isotope effects consistent with rate-limiting deprotonation ($k_H/k_D \geq 12$). The figure captions indicate when deuterated substrates were employed, but the deuteria are omitted from ChemDraw depictions and discussions to minimize visual clutter.

Reactions under standard synthetic conditions with only a moderate excess of NaHMDS show no anomalous curvatures that would be emblematic of autocatalysis or autoinhibition.[22a] Monitoring enolizations using [^{15}N]NaHMDS by ^{29}Si NMR spectroscopy showed no evidence of sodium enolate−NaHMDS mixed aggregates.[17]

Density functional theory (DFT) computations to probe experimentally elusive details were carried out at the M06-2X level of theory.[40,41] Monte Carlo conformational searches were performed with the molecular mechanics force field implemented in Spartan V8. The standard Def2-SVP basis set was used for geometric optimizations and the expanded Def2-TZVP basis set, for single point calculations.[42,43] Prompted by a recent publication revealing consequential free energy changes with larger integration grid sizes,[44] geometric optimizations and single-point calculations employed a refined (99 590) grid. Goodvibes (v3.0.1) was also used to streamline the extraction of thermochemical data.[45] During these studies, we have found that the calculations of either anionic or cationic fragments were unreliable even when isodesmic comparisons could, in principle, cancel large correlation errors.[46] Using the latest functionals from Head-Gordon (ωB97X-D), which include dispersion corrections and Dunning's diffuse function augmented basis set (aug-cc-pVTZ), showed closer alignment with the experimental data but were still inadequate.[47] A large number of DFT-computed energies of such ions are archived in the Supporting Information.

NaHMDS/Et_3N. Enolizations in toluene suffered from precipitation of some form of the enolate at low percent conversions,[48] prompting us to turn to the next weakest ligand, Et_3N. Plotting k_{obsd} versus the concentration of Et_3N in toluene measured at −78 °C (Figure 1) shows saturation kinetics consistent with the near quantitative displacement of the coordinated toluene to form complex **13a** (S = Et_3N). Saturation occurs at lower concentrations of Et_3N than for the double substitution on toluene-solvated NaHMDS dimer **1** to form dimer **2** owing to beneficial cooperative ketone−Et_3N solvation.[49] The linear rise at >1.0 M Et_3N shows a first-order dependence on free Et_3N.

Plotting k_{obsd} versus NaHMDS concentration (Figure 2) displays zeroth-order dependencies at both low and high Et_3N concentrations (2.0 and 7.0 M) expected for a reaction originating from **13a** (Mechanism E and eqs 19 and 20). Recall that a monomer-based metalation from an observable dimer (Mechanism F and eqs 21−23) would display an inverse half-order NaHMDS dependence. The rate data in total are consistent with Mechanism E in which the substantial extrapolated nonzero intercept of the linear Et_3N dependence corresponds to enolization via monosolvated dimer, A_2NaSK (**15**), and the Et_3N-dependent term corresponds to enolization via a disolvated dimer, A_2NaS_2K (**16**, Scheme 2). DFT

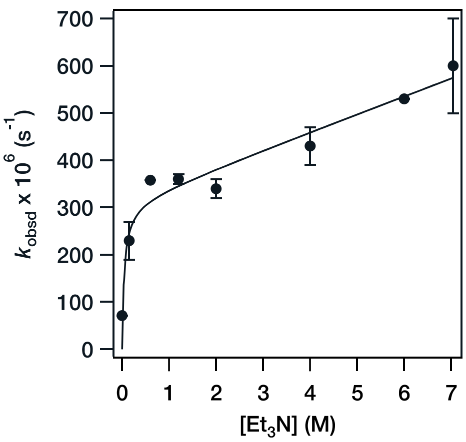

Figure 1. Plot of k_{obsd} vs [Et_3N] (M) for the enolization of 2-methyl-3-pentanone (**8**-d_0,0.005 M) by NaHMDS (0.10 M) in toluene at −78 °C measured by IR spectroscopy (1712 cm^{-1}). The curve is fit to a function that includes provisions for saturation kinetics leading to a first-oder dependence as described in the Supporting Information.

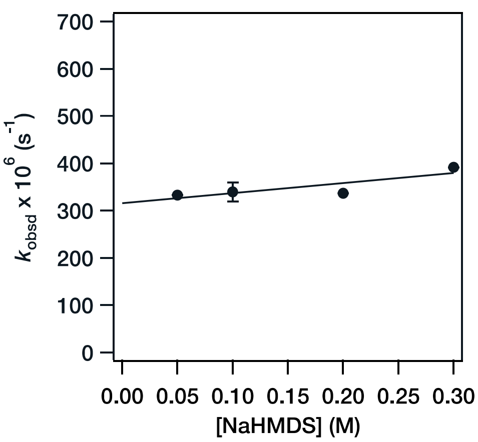

Figure 2. Plot of k_{obsd} vs [NaHMDS] (M) for the enolization of 2-methyl-3-pentanone (**8**-d_0, 0.005 M) by NaHMDS in 2.0 M Et_3N with toluene cosolvent at −78 °C measured with IR spectroscopy (1712 cm^{-1}). The curve depicts an unweighted least-squares fit to $y = ax + b$ [$a = (2.1 \pm 0.9) \times 10^4$; $b = (3.2 \pm 0.2) \times 10^4$].

Scheme 2. NaHMDS/Et_3N-Mediated Enolization of Ketone 8

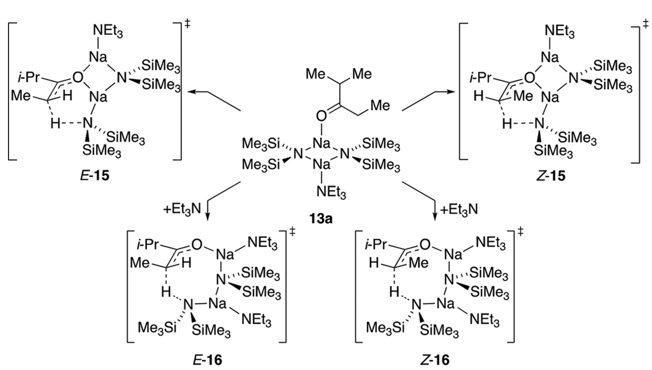

computations of the *E*- and *Z*-selective dimer-based transition structures in Figure 3 reflect the experimentally observed penchant for *E*-selective enolization that is higher for the disolvate.

https://doi.org/10.1021/jacs.1c06529
J. Am. Chem. Soc. 2021, 143, 17452−17464

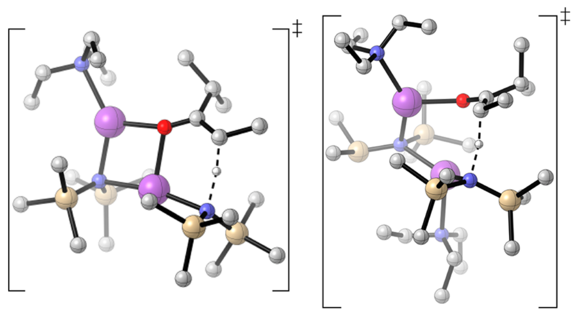

Figure 3. *E*-selective transition structures for the NaHMDS/Et_3N-based mono- and disolvated dimer (*E*-**15** and *E*-**16**).

NaHMDS/MTBE. IR spectroscopy of ketone−NaHMDS mixtures shows a slightly perturbed IR absorbance (1712 cm^{-1}) at low MTBE concentrations (see **13b**; S = MTBE) that becomes indistinguishable from free ketone (1718 cm^{-1}) at ≥2.0 M MTBE.[50] A plot of k_{obsd} versus NaHMDS concentration reveals a one-fourth-order dependence. In literally hundreds of rate laws determined for lithium amides,[23] we have never obtained an order that even approximated one-fourth. Plotting k_{obsd} versus MTBE concentration reveals a 1.6-order dependence on MTBE displaying a visible upward curvature, which is within experimental error of an idealized 1.5 order. Taken together, the rate data implicate the dimer-to-free ion pathway described by Mechanism H (eqs 27−29) and Scheme 3. DFT computed transition structures are archived in the Supporting Information.[46]

Scheme 3. NaHMDS/MTBE-Mediated Enolization of Ketone 8

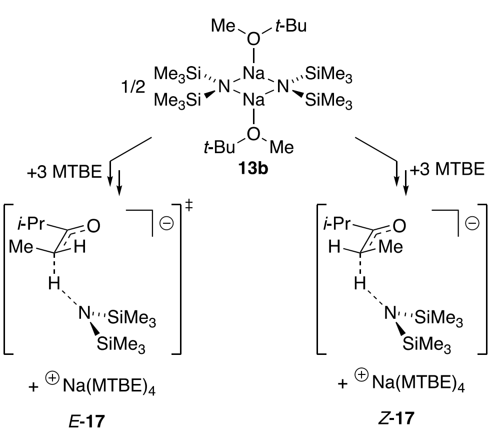

Guided by experience with lithium amides and the results for NaHMDS/THF (below), such a free ion-based mechanism in a nonpolar solvent is surprising. Nonetheless, the mobility of alkali metal ions in Et_2O is high,[51] and the $^+Na(MTBE)_4$ counterion is structurally precedented.[52] It is notable, however, that the reaction is slow in MTBE (Table 1). Therefore, one should focus less on how favorable the free ion-based mechanism is per se but on the inferiority of the alternative monomer- or dimer-based mechanisms. They must be problematic.

NaHMDS/*N,N,N′,N″,N″*-Pentamethyldiethylenetriamine (PMDTA). Enolization by NaHMDS/PMDTA manifests a half-order NaHMDS dependence accompanied by a half-order PMDTA dependence. In total, the data demand a full ionization of observable monomer κ^3-**7** as in Mechanism C (eqs 9−11). We had observed solvent-separated ion pair formation in the spectroscopic studies of NaHMDS[18] but were not able to spectroscopically distinguish them from free ions, which are suggested to be present in low concentrations based on dissociation constants of ion pairs.[24,53] An ion pair-based pathway (Mechanism B) and free ion-based pathway (Mechanism C), however, would display distinctly different rate laws. The free ion-based enolization is illustrated in Scheme 4.

Scheme 4. NaHMDS/PMDTA-Mediated Enolization of Ketone 8

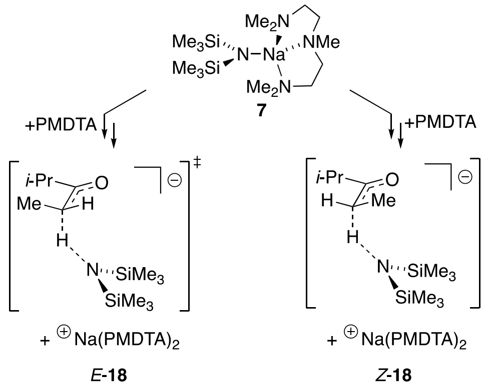

We previously computed both homo- and heterosolvates of sodium cations as part of the structural studies of NaHMDS, but we never considered $^+Na(PMDTA)_2$ because PMDTA seemed poorly suited as a *second* ligand.[19,54,55] Four denticities for the doubly solvated sodium counterions in Scheme 4 are represented as **19a−d** (Chart 2).[46] Ions **19c** and **19d** are structurally precedented.[56]

Chart 2. $^+Na(PMDTA)_2$ Counterions with Differing Denticities

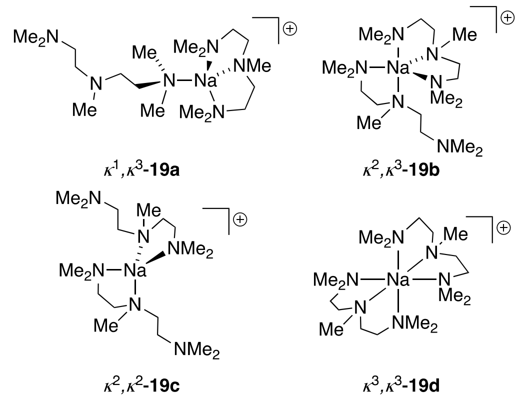

To probe the structure of the sodium counterion experimentally, we examined Me_2NEt and TMEDA as κ^1 and κ^2 surrogates, respectively, for the second PMDTA.[56] We surmised that mixed solvate **20** could mimic four-coordinate cation **19a** whereas mixed solvate **21** would mimic five-coordinate cation **19b**. Holding the PMDTA concentration fixed and varying the concentration of added Me_2NEt shows that Me_2NEt has little influence on the rate, affirming that **20** and, by proxy, **19a** are unimportant. The same experiment with TMEDA was predicted to track the half-order dependence on

Scheme 5. TMEDA-Mediated Enolizations from Monomer- and Dimer-Based Resting States

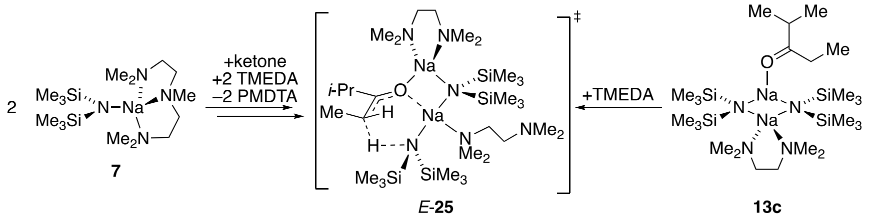

PMDTA owing to the intervention of **21** *if* PMDTA-solvated cation **19b** is important. An unexpected *second*-order TMEDA dependence was observed instead, which undermined the control experiment, left the cations **19b−d** indistinguishable, and foreshadowed a completely different mechanistic pathway.

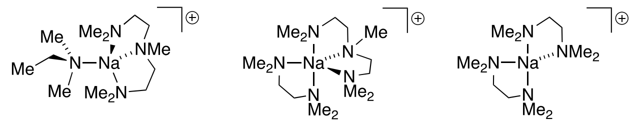

20 κ^3−$^+$Na(PMDTA)(DMEA) **21** κ^2,κ^3−$^+$Na(PMDTA)(TMEDA) **22** κ^2,κ^2−$^+$Na(TMEDA)$_2$

NaHMDS/TMEDA. We surmised from the aforementioned second-order TMEDA dependence that TMEDA must substitute for PMDTA, affording an isostructural variant of transition structure **18** bearing a $^+$Na(κ^2-TMEDA)$_2$ counterion (**22**). This was shown to be wrong when a *second-order dependence* on the observable PMDTA monomer **7** emerged. Taken together, the rate data were consistent with the generalized Mechanism I (eqs 30−32) in which two monomers associate to form a reactive dimer. Because structural studies clearly showed that PMDTA is more strongly bound than TMEDA, PMDTA must also act as an inhibitor. Indeed, identical conditions but with the omission of PMDTA resulted in a 5-fold acceleration. This called for an independent rate study of NaHMDS/TMEDA. IR spectra showed ketone **8**-d_3 observably complexes to NaHMDS in TMEDA/toluene. In principle, the complexed form could be either monomer **23a** or dimer **24a**. Owing to the rapid enolization, we were unable to unassailably detect either complex by ^{29}Si NMR spectroscopy; using DMPU as a surrogate showed a resonance at −15.2 ppm and $^1J_{N-Si}$ of 8.1 Hz that is fully characteristic of dimer **24b**, *not* monomer **23b**. We are fully comfortable concluding that ketone **8** drives TMEDA-solvated monomer **6** to mixed solvated dimer **24a**. Computations show a marked (10 kcal/mol) preference for ketone complexed dimer **24a** relative to **23a**.

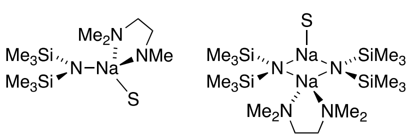

23a; S = ketone **23b**; S = DMPU **24a**; S = ketone **24b**; S = DMPU

Rate studies in TMEDA/toluene showed a zeroth-order NaHMDS dependence and first-order TMEDA dependence, consistent with Mechanism F (eqs 19 and 20; $n = 1$) involving a disolvated dimer. Thus, NaHMDS/TMEDA-mediated metalations, whether starting from PMDTA-solvated monomer **7** or complexed dimer **24a** converge on a common transition structure of stoichiometry $A_2Na_2S_2K$ (Scheme 5). Although DFT computations of transition structures bearing two κ^2-TMEDA ligands failed numerous attempts to converge, computed *E*- and *Z*-selective dimer-based transition structures with κ^1-TMEDA and κ^2-TMEDA ligands are illustrated in Figure 4. We remain unconvinced that κ^1-TMEDA is necessarily correct.

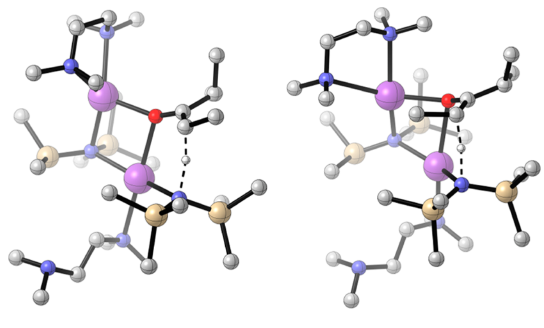

E-**25** *Z*-**25**

Figure 4. Transition structures for the NaHMDS dimer-based enolizations (*E*-**25** and *Z*-**25**) with κ^1-TMEDA and κ^2-TMEDA. The unassociated sodium cation is omitted.

The convergent mechanisms in Scheme 5 require context. Using PMDTA to establish a well-characterized resting state and to inhibit the reaction making it more tractable has potential importance as a tactical kinetic strategy. The associative mechanism involving the monomer-to-dimer pathway is unusual but has precedent,[28] including in the chemistry of TMEDA- and Et_3N-solvated LiHMDS.[19b,29,50] It is also unorthodox that a renowned chelating ligand, TMEDA, elicits a reaction via a higher aggregate, although years ago we realized that TMEDA's capacity to strongly chelate is highly contextual.[57] Pushing a TMEDA-solvated monomer to a dimer by the addition of an ostensibly weaker monofunctional ligand (ketone in this case) has also been observed for LiHMDS/TMEDA and certainly derives some driving force from cooperative solvation within the complexed dimer **24**.[18b,29] The general phenomenon in which the convergence of distinctly different resting states to a common (or at least isostructural) transition state was accompanied by markedly different rate behavior was observed for LiTMP-mediated epoxide eliminations.[58]

NaHMDS/THF. Enolizations of **8**-d_3 in THF/toluene with previously characterized tetrasolvated monomer **4** (Chart 1) implicate competing pathways involving a hexasolvated free ion and pentasolvated ion pair (**26** and **27**, Scheme 6).[59] A plot of k_{obsd} versus NaHMDS order stemming from a polynomial fit affords an order of 0.74 ± 0.07, suggesting the superposition of mechanisms involving free ions (Mechanism C) and either monomers (Mechanism A, eqs 3−5) or ion pairs (Mechanism B, eqs 6−8). A plot of k_{obsd} versus THF concentration manifests an upwardly curving THF dependence (1.3 order). An $ANaS_5$-based monomer seems unlikely, prompting our preference for

Scheme 6. NaHMDS/THF-Mediated Enolization of Ketone 8 via *Kinetic* Control

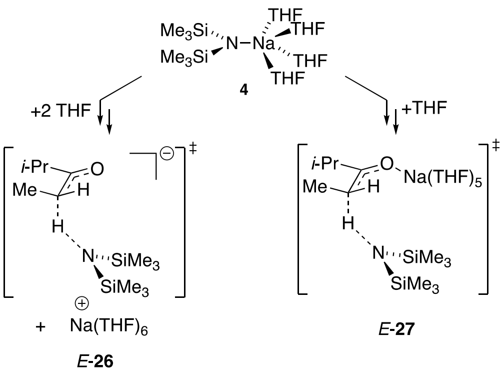

the ion pair **27**. Of the many arithmetic oddities discussed above, one of the least intuitive is that both the $ANaS_5$-based ion pair (Mechanism B) and the A^- and $^+NaS_6$ free ions (Mechanism C) predict first-order dependencies on the THF concentration because of the square root in eq 11 but not eq 8. As to the origin of the upward curvature, an analogy to lithium amides suggests a modest medium effect is to be expected.[23]

Free ion-based transition structure **26** differs from *E*-**18** (Scheme 4) only in the structure of the uncorrelated (free) sodium cation. Attempts to compute pentasolvated ion-paired transition structures *E*-**27** and *Z*-**27** afforded a valid saddle only for the latter. Recall, however, that the high *Z* selectivity for NaHMDS/THF arises from facile equilibration of the enolate.

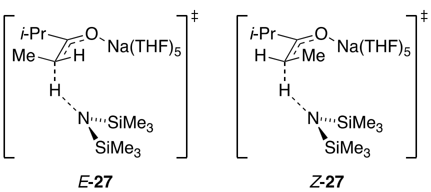

2-Methylcyclohexanone: NaHMDS/THF. At the outset, we pondered using 2-methylcyclohexanone (**11**) to solve some minor technical problems, presuming that **11** should be a surrogate of ketone **8**. This was deceptively underscored in eq 2. Rate studies revealed an *inverse-first-order* THF dependence and a first-order NaHMDS dependence. The rate data are consistent with monomer-based Mechanism A (eqs 3–5) with a requisite dissociation of one THF ($n = -1$) to allow binding of the ketone (eq 35). The calculated trisolvated-monomer-based transition structure (**28**) is illustrated in Figure 5.

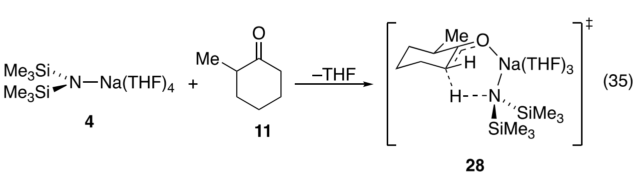

Curiously, ketone **11** undergoes monomer-based enolization whereas **8** does not. We thought that this would trace to their relative binding energies in which the added steric demands render **8** a relatively poor ligand (eq 36).

One of the harsh realities noted in the synopsis of Mechanism C is that we cannot exclude a triple ion-based transition structure such as **29** manifesting a free (uncorrelated) sodium cation. We have yet to design an experiment to resolve this.

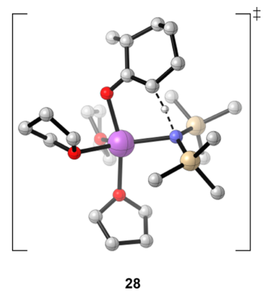

Figure 5. DFT-calculated transition structure **28** for the NaHMDS/THF-solvated enolization of 2-methylcyclohexanone (**11**).

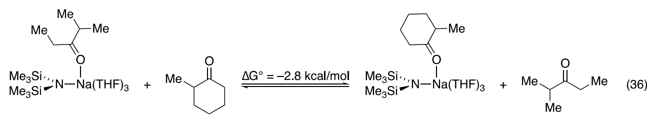

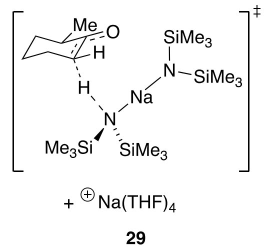

■ CONCLUSION

NaHMDS resides in the pantheon of amide bases alongside LiHMDS, LDA, and LiTMP. The almost 2000-fold range of *E*–*Z* enolization selectivities and >800-fold range of relative rates summarized in Table 1 match or exceed those of its competitors. The examination of what is seemingly a simple reaction for a small selection of standard solvents revealed four general mechanistic categories based on dimers, monomers, ion pairs, and free ions (Scheme 7). (Triple ions cannot be excluded in several instances.) The total count approaches nine mechanisms if one accounts for variable solvation numbers and NaHMDS resting states. This is a stupefying number of mechanisms at first blush, and we suspect we would find more by simply scrutinizing more solvents. In some sense, however, the unprecedented

Scheme 7. Mechanistic Summary

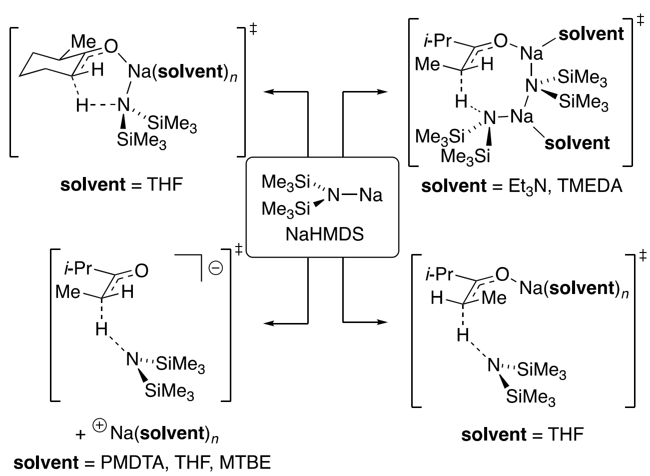

complexity is an artifact of examining so many diverse solvents in a single paper. Studies of LiHMDS and LDA have, when taken in total, produced their own bewildering array of mechanistic pathways and generated exceptionally complex mechanistic landscapes even in highly focused studies including enolizations.[23] LiHMDS-mediated enolization of oxazolidinones[60] or LDA-mediated reactions under nonequilibrium conditions[22a] manifests comparable complexity. Nonetheless, even the seemingly minor changes in solvent or substrate elicited a new mechanism for NaHMDS-mediated enolization at every turn. One positive feature is that it generated what we think is a pedagogically instructive tutorial on the relationships of concentration dependencies, rate laws, and mechanisms that we cordoned off in the prefacing Background section for the kinetically inclined. For the computationally inclined, we were disappointed to find that the computations of the ions, even when isodesmicity was rigorously maintained hoping for large electron correlation errors to cancel, produced results that often made no sense.[46]

We inadvertently stumbled back into the chemistry of sodium enolates when seemingly simple control experiments led to a protracted study of the THF-mediated *E*−*Z* equilibration. The *E*−*Z* equilibration in THF *without* isotopic exchanges reminds us of a number of oddities uncovered in the alkali metal world. These include Cram and Gosser's conducted tour mechanism,[61] Walborski et al.'s base-mediated epimerizations without isotopic exchanges,[62] Seebach et al.'s failures to deuterate enolates generated from LDA,[63] Kawabata and Fuji's amino acid-derived enolate alkylations that retain the memory of the configuration,[64] and even Davis et al.'s enolates generated with LDA in the presence of water.[65] They may somehow come together by our repeated observations that kinetically generated enolate aggregates can be remarkably slow to equilibrate.[34] The habit of letting reactions "warm to room temperature" may be covering over considerable complexity.

As we attempt to examine the guiding principles of how organosodium aggregation and solvation influence reactivities, one of our biggest challenges is to overcome our biases, constantly reminding ourselves that sodium is not lithium. The ligands required to optimize alkali metal chemistry are likely to be metal dependent. Almost four decades of experience studying organolithium structure−reactivity relationships did not prepare us for a few of the surprises. For example, a trivial change from 2-methyl-3-pentanone to isosteric 2-methylcyclohexanone produced a profound change in the mechanism. A free ion-based enolization using NaHMDS solvated by the weakly coordinating MTBE could not have been further from the expectation. On the other extreme, the addition of TMEDA to the NaHMDS/PMDTA monomer diverted a NaHMDS/PMDTA free ion-based enolization to a more efficient NaHMDS/TMEDA *dimer*-based enolization, which was equally unexpected. The two latter observations taken together fly in the face of all conventional wisdom.

Comparison of NaHMDS to LiHMDS is instructive. Their reactivities are highly solvent dependent, in some cases inverting their relative reactivities as highlighted in the Introduction. We suspect that many would not doubt the propensity of NaHMDS to ionize and attain higher overall solvation numbers when compared with LiHMDS. Comparisons of structural and rate studies of the two bases, however, find little tangible support for such assertions. The octahedral lithium cation is well documented,[66] for example, and the NaHMDS structures in Chart 1 all have structural analogs in LiHMDS.[50] Whether facile ionization of NaHMDS is to be exploited or avoided through the judicious choice of solvents is altogether unclear. It will likely depend on the application.

In this context, we are calling out synthetic chemists to stop using THF as the first and only resort. Of the almost 300 *E*−*Z* selectivities generated from NaHMDS easily detected in a database search, they were *all* in THF, the one solvent in which enolate equilibration was unstoppable. *There are other solvents.* NaHMDS is commercially available in toluene and easily prepared in almost any solvent. While NaHMDS/Et_3N fell short of our expectations based on LiHMDS/Et_3N,[19] the underestimate of potential applications of this inexpensive combination might be an error. We also must confess that it is tempting to probe KHMDS because, to put it bluntly again, potassium is not sodium either.

We are encouraged that NaHMDS offers insights into the role of sodium ion solvation as *molecular phenomena* rather than just generalized medium effects. Understanding sodium ion solvation is an important milestone and may have implications and applications outside of organic synthesis (such as sodium batteries).[67] Taking a broader view, it seems self-evident that understanding *any* subdiscipline of organometallic chemistry, not just the alkali metals, requires mapping the coordination and cooperation by *all* potential ligands, which includes the solvent.

■ EXPERIMENTAL SECTION

Reagents and Solvents. NaHMDS and [^{15}N]NaHMDS were prepared as white crystalline solids from hexamethyldizilazane and sodium metal.[18] Toluene, hexanes, THF, MTBE, PMDTA, and diglyme were distilled from blue or purple solutions containing sodium benzophenone ketyl. Ketone substrates were dried over 4 Å mol sieves.

NMR Spectroscopic Analyses. An NMR tube under vacuum was flame-dried on a Schlenk line, allowed to cool to room temperature, backfilled with argon, placed in a −78 °C dry ice/acetone bath, and charged with NaHMDS and solvents using stock solutions. The sample was mixed with a vortex mixer. Standard ^{1}H, ^{13}C, ^{15}N, and ^{29}Si spectra were recorded on a 500 MHz spectrometer at 500, 125.79, 50.66, and 99.36 MHz, respectively. The chemical shifts are referenced at −120 °C as follows: ^{1}H (Me_4Si, 0.0 ppm), ^{13}C (Me_4Si, 0.0 ppm), ^{15}N (neat Me_2NEt, 25.7 ppm), and ^{29}Si (Me_4Si, 0.0 ppm).

Rate Studies. IR spectra were recorded with an in situ IR spectrometer fitted with a 30-bounce, silicon-tipped probe. The spectra were acquired every 6 s from 16 scans at a gain of 1 and a resolution of 4 cm^{-1}. A representative reaction was carried out as follows: The IR probe was inserted through a nylon adapter and O-ring seal into an oven-dried, cylindrical flask fitted with a magnetic stir bar and a T-joint. The T-joint was capped with a septum for injections and a nitrogen line. After evacuation under full vacuum, heating, and flushing with nitrogen, the flask was charged with a 0.10 M stock solution of NaHMDS and cooled to −78 °C in dry ice−acetone using fresh acetone daily. After a background spectrum was recorded, ketone **8**-d_3 (0.028 mmol) in toluene (100 μL) was monitored with the absorbance at ketone **8**-d_3 at (1714 cm^{-1}) and enolate **9**-d_2 (1599 cm^{-1}).

Preparative-Scale Synthesis of NaHMDS/Et_3N (Unpurified). To a 100 mL three-neck round-bottom flask fitted with a magnetic stir bar was added sliced sodium metal (1.03 g, 45.0 mmol), 20 mL of Et_3N, and HMDS (7.31 g, 9.45 mL, 45.0 mmol) at rt. Isoprene (2.25 mL, 22.5 mmol) dissolved in 7.75 mL of dry Et_3N was then added over 1 h via a syringe pump. The reaction was stirred at room temperature for an additional 2 h. The solution was subsequently transferred by cannula to a 50 mL flask fitted with a T-joint. Titration[68] showed the solution to be 0.97 M. ^{1}H NMR spectrum (500 MHz, Et_3N) δ −0.02 ppm; ^{13}C NMR spectrum (125.72 MHz, Et_3N) δ 6.5 ppm; ^{29}Si NMR spectrum (99.36 MHz, Et_3N) δ −14.5 ppm.

https://doi.org/10.1021/jacs.1c06529
J. Am. Chem. Soc. 2021, 143, 17452−17464

■ ASSOCIATED CONTENT

Supporting Information

The Supporting Information is available free of charge at https://pubs.acs.org/doi/10.1021/jacs.1c06529.

Spectroscopic, rate, and computational data (PDF)

■ AUTHOR INFORMATION

Corresponding Author

David B. Collum − *Department of Chemistry and Chemical Biology Baker Laboratory, Cornell University, Ithaca, New York 14853-1301, United States;* orcid.org/0000-0001-6065-1655; Email: dbc6@cornell.edu

Author

Ryan A. Woltornist − *Department of Chemistry and Chemical Biology Baker Laboratory, Cornell University, Ithaca, New York 14853-1301, United States*

Complete contact information is available at: https://pubs.acs.org/10.1021/jacs.1c06529

Notes

The authors declare no competing financial interest.

■ ACKNOWLEDGMENTS

We thank the National Institutes of Health (GM131713) for support.

■ REFERENCES

(1) Woltornist, R. A.; Ma, Y.; Algera, R. F.; Zhou, Y.; Zhang, Z.; Collum, D. B. Structure, Reactivity, and Synthetic Applications of Sodium Diisopropylamide. *Synthesis* **2020**, *52*, 1478.

(2) (a) Seyferth, D. Alkyl and Aryl Derivatives of the Alkali Metals: Useful Synthetic Reagents as Strong Bases and Potent Nucleophiles. 1. Conversion of Organic Halides to Organoalkali-Metal Compounds. *Organometallics* **2006**, *25*, 2. (b) Seyferth, D. Alkyl and Aryl Derivatives of the Alkali Metals: Strong Bases and Reactive Nucleophiles. 2. Wilhelm Schlenk's Organoalkali-Metal Chemistry. The Metal Displacement and the Transmetalation Reactions. Metalation of Weakly Acidic Hydrocarbons. Superbases. *Organometallics* **2009**, *28*, 2. (c) Lochmann, L.; Janata, M. 50 Years of Superbases Made from Organolithium Compounds and Heavier Alkali Metal Alkoxides. *Eur. J. Chem.* **2014**, *12*, 537. (d) Robertson, S. D.; Uzelac, M.; Mulvey, R. E. Alkali-Metal-Mediated Synergistic Effects in Polar Main Group Organometallic Chemistry. *Chem. Rev.* **2019**, *119*, 8332.

(3) For an extensive review of the chemistry of the alkali metal amides, see: Mulvey, R. E.; Robertson, S. D. Synthetically Important Alkali-Metal Utility Amides: Lithium, Sodium, and Potassium Hexamethyldisilazides, Diisopropylamides, and Tetramethylpiperidides. *Angew. Chem., Int. Ed.* **2013**, *52*, 11470.

(4) (a) Stumpf, A.; Cheng, Z. K.; Wong, B.; Reynolds, M.; Angelaud, R.; Girotti, J.; Deese, A.; Gu, C.; Gazzard, L. Development of an Expedient Process for the Multi-Kilogram Synthesis of Chk1 Inhibitor GDC-0425. *Org. Process Res. Dev.* **2015**, *19*, 661. (b) Kerdesky, F. A. J.; Leanna, M. R.; Zhang, J.; Li, W.; Lallaman, J. E.; Ji, J.; Morton, H. E. An Efficient Multikilogram Synthesis of ABT-963: A Selective COX-2 Inhibitor. *Org. Process Res. Dev.* **2006**, *10*, 512. (c) Davis, F. A. Recent Applications of *N*-Sulfonyloxaziridines (Davis oxaziridines) in Organic Synthesis. *Tetrahedron* **2018**, *74*, 3198.

(5) (a) Jost, S.; Günther, H. ^{13}C and ^{23}Na Solid-state NMR Spectra of Organosodium Compounds. *Magn. Reson. Chem.* **2003**, *41*, 373. (b) McMillen, C. H.; Gren, C. K.; Hanusa, T. P.; Rheingold, A. L. A Tetrameric Allyl Complex of Sodium, and Computational Modeling of the ^{23}Na−Allyl Chemical Shift. *Inorg. Chim. Acta* **2010**, *364*, 61. (c) Pakuro, N. I.; Arest-Yakubovich, A. A.; Shcheglova, L. V.; Petrovsky, P. V.; Chekulaeva, L. A. NMR Spectra of a Hydrocarbon-Soluble Organosodium Compound and Its Lithium Analogs. *Russ. Chem. Bull.* **1996**, *45*, 838. (d) Delville, A.; Detellier, C.; Gerstmans, A.; Laszlo, P. Chelation of the Sodium Cation by Polyamines: A Novel Approach to Preferential Solvation and to the Understanding of Sodium-23 Chemical Shifts and Quadrupolar Coupling Constants. *J. Am. Chem. Soc.* **1980**, *102*, 6558. (e) Boche, G.; Etzrodt, H. The Reaction of *n*-Butyllithium/sodium(potassium) *tert*-Butoxide (Lochmann-Schlosser Base) with a CH-Acid Leads to Organosodium(potassium) Compounds. An NMR Spectroscopical Study of Several Organolithium, -sodium and -potassium Compounds in Tetrahydrofuran-d_2. *Tetrahedron Lett.* **1983**, *24*, 5477.

(6) (a) Nakhmanovich, B. I.; Zolotareva, I. V.; Litvinenko, G. I.; Arest-Yakubovich, A.; Muller, A. H. E. Anionic Polymerization of Butadiene Initiated by Tributyltin Sodium. Kinetic Analysis of Induction Periods Generated by Transfer to Initiator Precursor. *Macromol. Chem. Phys.* **2001**, *202*, 3536. (b) Alvarino, J. M. Structure of the Ionic Species in Organosodium Compounds Dissolved in n-Electron Donor, Low Dielectric Constant Media. *J. Organomet. Chem.* **1975**, *90*, 133. (c) Ahlberg, P.; Karlsson, A.; Davidsson, O.; Hilmersson, G.; Loewendahl, M. Mechanism and Solvent Catalysis of the Degenerate 1,12-Metalations of [1.1]Ferrocenophanyllithium and [1.1]-Ferrocenophanylsodium Studied by NMR Spectroscopy. *J. Am. Chem. Soc.* **1997**, *119*, 1751.

(7) (a) Schleyer, P. v. R.; Clark, T.; Kos, A. J.; Spitznagel, G. W.; Rohde, C.; Arad, D.; Houk, K. N.; Rondan, N. G. Structures and Stabilities of α-Hetero-Substituted Organolithium and Organosodium Compounds. Energetic Unimportance of Second-Row d-Orbital Effects. *J. Am. Chem. Soc.* **1984**, *106*, 6467. (b) Papadopoulos, M. G.; Raptis, S. G. Organolithium and Organosodium Compounds: the Second Hyperpolarizabilities of $C_8H_6Li_2$ and $C_8H_6Na_2$. *Mol. Phys.* **1997**, *92*, 547. (c) Sabirov, Z. M.; Manakov, Yu. B.; Ponomarev, O. A.; Minsker, K. S.; Rafikov, S. R. Theoretical Study of the Structure and Reactivity of Active Centers During Anionic Polymerization of Unsaturated Nonpolar Monomers. *Zh. Fiz. Khim.* **1985**, *59*, 1136. (d) Sulway, S. A.; Girshfeld, R.; Solomon, S. A.; Muryn, C. A.; Poater, J.; Solà, M.; Bickelhaupt, F. M.; Layfield, R. A. Alkali Metal Complexes of Silyl-Substituted ansa-(Tris)allyl Ligands: Metal-, Co-Ligand- and Substituent-Dependent Stereochemistry. *Eur. J. Inorg. Chem.* **2009**, *2009*, 4157. (e) Majhi, J.; Turnbull, B. W. H.; Ryu, H.; Park, J.; Baik, M.-H.; Evans, P. A. Dynamic Kinetic Resolution of Alkenyl Cyanohydrins Derived from α,β-Unsaturated Aldehydes: Stereoselective Synthesis of E-Tetrasubstituted Olefins. *J. Am. Chem. Soc.* **2019**, *141*, 11770. (f) Also, see ref 5b.

(8) *n*-BuNa and related alkylithiums[9−11] as well as NaDA and various sodium dialkylamides[12] are easily prepared and solubilized. *n*-BuNa affords stock solutions in *N,N*-dimethylethylamine (DMEA) that are stable with refrigeration (unpublished).

(9) (a) Schade, C.; Bauer, W.; Schleyer, P. v. R. *n*-Butylsodium: The Preparation, Properties and NMR Spectra of a Hydrocarbon- and Tetrahydrofuran-Soluble Reagent. *J. Organomet. Chem.* **1985**, *295*, c25−c28. (b) Turner, R. R.; Altenau, A. G.; Cheng, T. C. Analysis of Butyllithium and Butylsodium in the Presence of Alkoxides. *Anal. Chem.* **1970**, *42*, 1835. (c) Majewski, M., Snieckus, V., Eds. Product Subclass 9: Allylsodium Compounds. In *Category 1, Organometallics*; Georg Thieme Verlag: Stuttgart, 2016. (d) Lochmann, L.; Pospíšil, J.; Lím, D. On the Interaction of Organolithium Compounds with Sodium and Potassium Alkoxides. A New Method for the Synthesis of Organosodium and Organopotassium Compounds. *Tetrahedron Lett.* **1966**, *7*, 257. (e) Clegg, W.; Conway, B.; Kennedy, A. R.; Klett, J.; Mulvey, R. E.; Russo, L. Synthesis and Structures of [(Trimethylsilyl)-methyl]sodium and -potassium with Bi- and Tridentate N-Donor Ligands. *Eur. J. Inorg. Chem.* **2011**, *2011*, 721. (f) Gilman, H.; Bebb, R. L. Relative Reactivities of Organometallic Compounds. XX. Metalation. *J. Am. Chem. Soc.* **1939**, *61*, 109. (g) Harenberg, J. H.; Weidmann, N.; Wiegand, A. J.; Hoefer, C. A.; Annapureddy, R. R.; Knochel, P. (2-Ethylhexyl)sodium: A Hexane-Soluble Reagent for Br/Na-Exchanges and Directed Metalations in Continuous Flow. *Angew. Chem., Int. Ed.* **2021**, *60*, 14296.

(10) We examined the efficacy of 2-ethylhexylsodium as a hydrocarbon soluble alkylsodium and found it functional but inconvenient to manipulate: (a) Eidt, S. H.; Malpass, D. B. Solutions of Sodium Alkyls in Hydrocarbons and Process for Preparing Said Solutions. Eur. EP0041306. *Chem. Abstr.* **1981**, *96*, 123007. (b) Sakharov, S. G.; Pakuro, N. I.; Arest-Yakubovich, A. A.; Shcheglova, L. V.; Petrovskii, P. V. NMR Study of the Dynamic Behaviour of the System 2-Ethylhexylsodium-2-ethylhexyllithium in Heptane. *J. Organomet. Chem.* **1999**, *580*, 205. (c) Maréchal, J.-M.; Carlotti, S.; Shcheglova, L.; Deffieux, A. Stereoregulation in the Anionic Polymerization of Styrene Initiated by Superbases. *Polymer* **2003**, *44*, 7601.

(11) Asako, S.; Takahashi, I.; Nakajima, H.; Ilies, L.; Takai, K. Halogen−Sodium Exchange Revisited. *Commun. Chem.* **2021**, *4*, 76.

(12) (a) Raynolds, S.; Levine, R. The Synthesis of Nitrogen-containing Ketones. VIII. The Acylation of 3-Picoline, 4-Picoline and Certain of their Derivatives. *J. Am. Chem. Soc.* **1960**, *82*, 472. (b) Lochmann, L.; Trekoval, J. Interactions of Alkoxides XI. Reactions of Substituted N-Lithium Amides with Heavier Alkali Metal Alkoxides. A Novel Method for the Preparation of N-Sodium and N-Potassium Dialkylamides. *J. Organomet. Chem.* **1979**, *179*, 123. (c) Barr, D.; Dawson, A. J.; Wakefield, B. J. A Simple, High-Yielding Preparation of Sodium Diisopropylamide and Other Sodium Dialkylamides. *J. Chem. Soc., Chem. Commun.* **1992**, 204. (d) Andrews, P. C.; Barnett, N. D. R.; Mulvey, R. E.; Clegg, W.; O'Neil, P. A.; Barr, D.; Cowton, L.; Dawson, A. J.; Wakefield, B. J. X-ray Crystallographic Studies and Comparative Reactivity Studies of a Sodium Diisopropylamide (NDA) Complex and Related Hindered Amides. *J. Organomet. Chem.* **1996**, *518*, 85.

(13) Watson, B. T.; Lebel, H. Sodium Hexamethyldisilazide. In *e-EROS Encyclopedia of Reagents for Organic Synthesis*; John Wiley & Sons: New York, 2005; p 1−10.

(14) (a) Butters, M.; Ebbs, J.; Green, S. P.; MacRae, J.; Morland, M. C.; Murtiashaw, C. W.; Pettman, A. J. Process Development of Voriconazole: A Novel Broad-Spectrum Triazole Antifungal Agent. *Org. Process Res. Dev.* **2001**, *5*, 28. (b) Fuerstner, A.; Fenster, M. D. B.; Fasching, B.; Godbout, C. P.; Radkowski, K. Toward the Total Synthesis of Spirastrellolide A. Part 2: Conquest of the Northern Hemisphere. *Angew. Chem., Int. Ed.* **2006**, *45*, 5510. (c) Rao, K. S.; St-Jean, F.; Kumar, A. Quantitation of a Ketone Enolization and a Vinyl Sulfonate Stereoisomer Formation Using Inline IR Spectroscopy and Modeling. *Org. Process Res. Dev.* **2019**, *23*, 945. (d) Also, see ref 4.

(15) (a) Driess, M.; Pritzkow, H.; Skipinski, M.; Winkler, U. Synthesis and Solid State Structures of Sterically Congested Sodium and Cesium Silyl(fluorosilyl)phosphanide Aggregates and Structural Characterization of the Trimeric Sodium Bis(trimethylsilyl)amide. *Organometallics* **1997**, *16*, 5108. (b) Kennedy, A. R.; Mulvey, R. E.; O'Hara, C. T.; Robertson, S. D.; Robertson, G. M. Catena-Poly[Sodium-μ_2-(*N,N,N′,N′*- Tetramethylethane-1,2-Diamine)-κ^2-*N,N′*-Sodium- Bis-[μ_2-Bis(Trimethylsilyl)Azanido-κ^2 *N:N*]]. *Acta Crystallogr., Sect. E: Struct. Rep. Online* **2012**, *68*, m1468. (c) Schüler, P.; Görls, H.; Westerhausen, M.; Kriec, S. Bis(trimethylsilyl)amide Complexes of s-Block Metals with Bidentate Ether and Amine Ligands. *Dalton Trans.* **2019**, *48*, 8966. (d) Ojeda-Amador, A. I.; Martínez-Martínez, A. J.; Kennedy, A. R.; Armstrong, D. R.; O'Hara, C. T. Monodentate Coordination of the Normally Chelating Chiral Diamine (*R,R*)-TMCDA. *Chem. Commun.* **2017**, *53*, 324. (e) Sarazin, Y.; Coles, S. J.; Hughes, D. L.; Hursthouse, M. B.; Bochmann, M. Cationic Brønsted Acids for the Preparation of Sn(IV) Salts: Synthesis and Characterisation of $[Ph_3Sn(OEt_2)][H_2N\{B(C_6F_5)_3\}_2]$,$[Sn(NMe_2)_3(HNMe_2)_2]$-$[B(C_6F_5)_4]$ and $[Me_3Sn(HNMe_2)_2][B(C_6F_5)_4]$. *Eur. J. Inorg. Chem.* **2006**, *2006*, 3211. (f) Karl, M.; Seybert, G.; Massa, W.; Harms, K.; Agarwal, S.; Maleika, R.; Stelter, W.; Greiner, A.; Neumüller, W. H.; Dehnicke, K. Amidometallate von Seltenerdelementen. Synthese Und Kristallstrukturen von $[Na(12\text{-Krone-}4)_2][M\{N(SiMe_3)_2\}_3(OSiMe_3)]$ (M = Sm, Yb), $[Na(THF)_3Sm\{N(SiMe_3)_2\}_3(C{\equiv}C\text{-Ph})]$, $[Na(THF)_6][Lu_2(\mu\text{-}NH_2)(\mu\text{-}NSiMe_3)\{N(SiMe_3)_2\}_4]$ Sowie von $[NaN(SiMe_3)_2(THF)]_2$. *Z. Anorg. Allg. Chem.* **1999**, *625*, 1301. (g) Neufeld, R.; Michel, R.; Herbst-Irmer, R.; Schöne, R.; Stalke, D. Introducing a Hydrogen-Bond Donor into a Weakly Nucleophilic Brønsted Base: Alkali Metal Hexamethyldisilazides (MHMDS, M = Li, Na, K, Rb, and Cs) with Ammonia. *Chem. - Eur. J.* **2016**, *22*, 12340. (h) Edelmann, F. T.; Pauer, F.; Wedler, M.; Stalke, D. Preparation and Structural Characterization of Dioxane Coordinated Alkali Metal Bis-(Trimethylsilyl)Amides. *Inorg. Chem.* **1992**, *31*, 4143.

(16) (a) Kupce, E.; Lukevics, E.; Varezhkin, Y. M.; Mikhailova, A. N.; Sheludyakov, V. D. Silicon-29-Nitrogen-15 Spin-Spin Coupling Constants in Silazanes. *Organometallics* **1988**, *7*, 1649. (b) Luo, G.; Luo, Y.; Qu, J. Direct Nucleophilic Trifluoromethylation Using Fluoroform: A Theoretical Mechanistic Investigation and Insight into the Effect of Alkali Metal Cations. *New J. Chem.* **2013**, *37*, 3274. (c) Also, see ref 15d.

(17) For examples of NaHMDS-derived mixed aggregates, see: (a) Knapp, C.; Lork, E.; Borrmann, T.; Stohrer, W.-D.; Mews, R. Versuche Zur Darstellung Vont-BuCN_5S_3 Und Die Unerwartete Isolierung Einer Kovalenten Modifikation von Tetraschwefelpentas-tickstoff-Chlorid S_4N_5Cl. *Z. Anorg. Allg. Chem.* **2005**, *631*, 1885. (b) Clark, N. M.; García-Álvarez, P.; Kennedy, A. R.; O'Hara, C. T.; Robertson, G. M. Reactions of (−)-Sparteine with Alkali Metal HMDS Complexes: Conventional Meets the Unconventional. *Chem. Commun.* **2009**, *39*, 5835. (c) Williard, P. G.; Nichols, M. A. Structural Characterization of Mixed Alkali Metal Bis(trimethylsilyl) Amide Bases. *J. Am. Chem. Soc.* **1991**, *113*, 9671. (d) Ojeda-Amador, A. I.; Martinez-Martinez, A. J.; Kennedy, A. R.; O'Hara, C. T. Synthetic and Structural Studies of Mixed Sodium Bis(trimethylsilyl) Amide/Sodium Halide Aggregates in the Presence of ν^2-*N,N*-, ν^3-*N,N,N/N,O,N*-, and ν^4-*N,N,N,N*-donor Ligands. *Inorg. Chem.* **2015**, *54*, 9833. (e) Williard, P. G.; Hintze, M. J. Crystal Structures of a Lithium Ketone Enolate/Lithium Amide and of a Sodium Ester Enolate/Sodium Amide. *J. Am. Chem. Soc.* **1990**, *112*, 8602.

(18) (a) Woltornist, R. A.; Collum, D. B. Using $^{15}N{-}^{29}Si$ Scalar Coupling to Determine Aggregation and Solvation States. *J. Am. Chem. Soc.* **2020**, *142*, 6852. (b) Woltornist, R. A.; Collum, D. B. Aggregation and Solvation of Sodium Hexamethyldisilazide: Across the Solvent Spectrum. *J. Org. Chem.* **2021**, *86*, 2406.

(19) (a) Godenschwager, P.; Collum, D. B. Lithium Hexamethyldisilazide-Mediated Enolizations: Influence of Triethylamine on E/Z Selectivities and Enolate Reactivities. *J. Am. Chem. Soc.* **2008**, *130*, 8726. (b) Mack, K. A.; McClory, A.; Zhang, H.; Gosselin, F.; Collum, D. B. Lithium Hexamethyldisilazide-Mediated Enolization of Highly Substituted Aryl Ketones: Structural and Mechanistic Basis of the E/Z Selectivities. *J. Am. Chem. Soc.* **2017**, *139*, 12182. (c) Zhao, P.; Collum, D. B. Ketone Enolization by Lithium Hexamethyldisilazide: Structural and Rate Studies of the Accelerating Effects of Trialkylamines. *J. Am. Chem. Soc.* **2003**, *125*, 14411. (d) Fulton, T. J.; Cusumano, A. Q.; Alexy, E. J.; Du, Y. E.; Zhang, H.; Houk, K. N.; Stoltz, B. M. Global Diastereoconvergence in the Ireland−Claisen Rearrangement of Isomeric Enolates: Synthesis of Tetrasubstituted α-Amino Acids. *J. Am. Chem. Soc.* **2020**, *142*, 21938.

(20) For extensive references and discussions of *E*- and *Z*-selective enolizations, see ref 19a.

(21) Edwards, J. O.; Greene, E. F.; Ross, J. From Stoichiometry and Rate Law to Mechanism. *J. Chem. Educ.* **1968**, *45*, 381.

(22) (a) Algera, R. F.; Gupta, L.; Hoepker, A. C.; Liang, J.; Ma, Y.; Singh, K. J.; Collum, D. B. Lithium Diisopropylamide: Non-Equilibrium Kinetics and Lessons Learned About Rate Limitation. *J. Org. Chem.* **2017**, *82*, 4513. (b) For an excellent discussion of the various isotope effects from a decidedly thermochemical perspective, see: Simmons, E. M.; Hartwig, J. F. On the Interpretation of Deuterium Kinetic Isotope Effects in C−H Bond Functionalizations by Transition-Metal Complexes. *Angew. Chem., Int. Ed.* **2012**, *51*, 3066. (c) Meek, S. J.; Pitman, C. L.; Miller, A. J. M. Deducing Reaction Mechanism: A Guide for Students, Researchers, and Instructors. *J. Chem. Educ.* **2016**, *93*, 275.

(23) Allusions to LDA can be traced to the original literature via the following review: Collum, D. B.; McNeil, A. J.; Ramírez, A. Lithium Diisopropylamide: Solution Kinetics and Implications for Organic Synthesis. *Angew. Chem., Int. Ed.* **2007**, *46*, 3002.

(24) Ashby, E. C.; Dobbs, F. R.; Hopkins, H. P., Jr. Composition of Complex Aluminum Hydrides and Borohydrides, as Inferred from

Conductance, Molecular Association, and Spectroscopic Studies. *J. Am. Chem. Soc.* **1973**, *95*, 2823.

(25) The enthalpic cost of separating a solvent-separated ion pair to free ions in THF is variable but has been estimated to be as low as 1−2 kcal/mol: Hogen-Esch, T. E.; Smid, J. *J. Am. Chem. Soc.* **1966**, *88*, 318.

(26) (a) For an extensive bibliography to triple ions, see: Ma, Y.; Algera, R. F.; Collum, D. B. Sodium Diisopropylamide in *N,N*-Dimethylethylamine: Reactivity, Selectivity, and Synthetic Utility. *J. Org. Chem.* **2016**, *81*, 11312. (b) We have described rate data supporting the intermediacy of lithium amide-based triple ions: Hoepker, A. C.; Gupta, L.; Ma, Y.; Faggin, M. F.; Collum, D. B. Regioselective Lithium Diisopropylamide-Mediated Ortholithiation of 1-Chloro-3-(trifluoromethyl)benzene: Role of Autocatalysis, Lithium Chloride Catalysis, and Reversibility. *J. Am. Chem. Soc.* **2011**, *133*, 7135.

(27) Ramírez, A.; Sun, X.; Collum, D. B. Lithium Diisopropylamide-Mediated Enolization: Catalysis by Hemilabile Ligands. *J. Am. Chem. Soc.* **2006**, *128*, 10326.

(28) For evidence of associations of monomers to dimers prior to the reaction, see ref 19b and the references cited therein.

(29) For leading references to the failed correlation of the aggregation state with solvent donicity using LiHMDS, see: Lucht, B. L.; Collum, D. B. Lithium Hexamethyldisilazide: A View of Lithium Ion Solvation Through a Glass-Bottom Boat. *Acc. Chem. Res.* **1999**, *32*, 1035.

(30) Me_3SiCl/Et_3N mixtures afford near quantitative enolate or carbanion trapping by centrifuging the quantitatively precipitated Et_3N-HCl: Stork, G.; Hudrlik, P. F. Isolation of Ketone Enolates as Trialkylsilyl Ethers. *J. Am. Chem. Soc.* **1968**, *90*, 4462.

(31) Gaudemar, M.; Bellassoued, M. Regio and Stereoselective Preparation of Enolates from Ketones by Means of Sodium Bis-(Trimethylsilyl)-Azide. *Tetrahedron Lett.* **1989**, *30*, 2779.

(32) Odd selectivities for LDA-mediated enolizations were traced to exclusively kinetic control. Xie, L.; Saunders, W. H., Jr. Unusual Induced Isotope Effects in the Reaction of 2-Pentanone with Dialkylamide Bases. Evidence on the Nature of the Reactive Base Species. *J. Am. Chem. Soc.* **1991**, *113*, 3123.

(33) The absorbances correspond to subunits in what is likely an ensemble of homo- and heterodimers.[19b]

(34) (a) Tallmadge, E. H.; Collum, D. B. Evans Enolates: Solution Structures of Lithiated Oxazolidinone-Derived Enolates. *J. Am. Chem. Soc.* **2015**, *137*, 13087. (b) Jin, K. J.; Collum, D. B. Solid-State and Solution Structures of Glycinimine-Derived Lithium Enolates. *J. Am. Chem. Soc.* **2015**, *137*, 14446.

(35) Taylor, S. L.; Lee, D. Y.; Martin, J. C. Direct, Regiospecific 2-Lithiation of Pyridines and Pyridine 1-Oxides with in situ Electrophilic Trapping. *J. Org. Chem.* **1983**, *48*, 4156.

(36) Rein, A. J.; Donahue, S. M.; Pavlosky, M. A. In Situ FTIR Reaction Analysis of Pharmaceutical-Related Chemistry and Processes. *Curr. Opin. Drug Discovery Dev.* **2000**, *3*, 734.

(37) In earlier studies of LiHMDS reporting a 1714 cm^{-1} shift of a ketone carbonyl,[19a] we *might* have inadvertently compared the free ketone with the bound deuterated analog while failing to account for isotopic shifts on the carbonyl absorbance.[39] Our measurements herein show NaHMDS/Et_3N-**8**-d_3 (1704 cm^{-1}) and free **8**-d_3 (1715 cm^{-1}).

(38) Nolin, B. R.; Jones, R. N. The Infrared Absorption Spectra of Diethyl Ketone and its Deuterium Substitution Products. *J. Am. Chem. Soc.* **1953**, *75*, 5626.

(39) Rivera-Gaines, V. E.; Leibowitz, S. J.; Laane, J. Far-Infrared Spectra, Two-Dimensional Vibrational Potential Energy Surface, and Conformation of Cyclohexene and Its Isotopomers. *J. Am. Chem. Soc.* **1991**, *113*, 9735.

(40) Frisch, M. J.; Trucks, G. W.; Schlegel, H. B.; Scuseria, G. E.; Robb, M. A.; Cheeseman, J. R.; Zakrzewski, V. G.; Montgomery, J. A., Jr.; Stratmann, R. E.; Burant, J. C.; Dapprich, S.; Millam, J. M.; Daniels, A. D.; Kudin, K. N.; Strain, M. C.; Farkas, O.; Tomasi, J.; Barone, V.; Cossi, M.; Cammi, R.; Mennucci, B.; Pomelli, C.; Adamo, C.; Clifford, S.; Ochterski, J.; Petersson, G. A.; Ayala, P. Y.; Cui, Q.; Morokuma, K.; Malick, D. K.; Rabuck, A. D.; Raghavachari, K.; Foresman, J. B.; Cioslowski, J.; Ortiz, J. V.; Baboul, A. G.; Stefanov, B. B.; Liu, G.; Liashenko, A.; Piskorz, P.; Komaromi, I.; Gomperts, R.; Martin, R. L.; Fox, D. J.; Keith, T.; Al-Laham, M. A.; Peng, C. Y.; Gill, A.; Nanayakkara, C.; Gonzalez, M.; Challacombe, P. M. W.; Johnson, B.; Chen, W.; Wong, M. W.; Andres, J. L.; Gonzalez, C.; Head-Gordon, M.; Replogle, E. S.; Pople, J. A. *Gaussian 09*, Revision A.02; Gaussian, Inc.: Wallingford, CT, 2009.

(41) Zhao, Y.; Truhlar, D. G. The M06 Suite of Density Functionals for Main Group Thermochemistry, Thermochemical Kinetics, Noncovalent Interactions, Excited States, and Transition Elements: Two New Functionals and Systematic Testing of Four M06-Class Functionals and 12 Other Functionals. *Theor. Chem. Acc.* **2008**, *120*, 215.

(42) Weigend, F.; Ahlrichs, R. Balanced Basis Sets of Split Valence, Triple Zeta Valence and Quadruple Zeta Valence Quality for H to Rn: Design and Assessment of Accuracy. *Phys. Chem. Chem. Phys.* **2005**, *7*, 3297.

(43) Legault, C. Y. *CYLview, 1.0b*; Université de Sherbrooke, 2009; http://www.cylview.org (accessed 2021−09−14).

(44) Bootsma, A. N.; Wheeler, S. Popular Integration Grids Can Result in Large Errors in DFT-Computed Free Energies *ChemRxiv* **2019**, DOI: 10.26434/chemrxiv.8864204.v5 (accessed 2021−09−14).

(45) Luchini, G.; Alegre-Requena, J. V.; Funes-Ardoiz, I.; Paton, R. S. GoodVibes: Automated Thermochemistry for Heterogeneous Computational Chemistry Data. *F1000Research* **2020**, *9*, 291.

(46) The following two examples are emblematic of what appears to be correlation error skewing isodesmic comparisons:

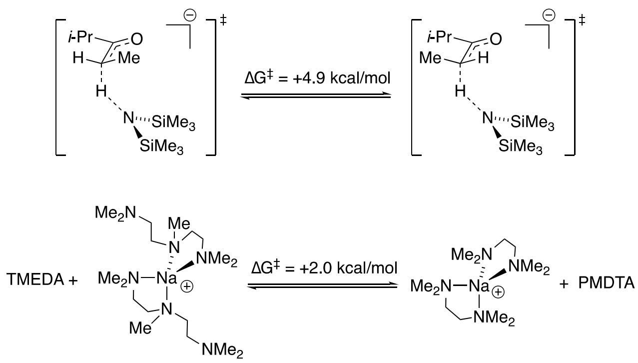

The former is contradicted by the experiment whereas the latter defies common sense. The inclusion of dispersion corrections and diffuse functions in a higher-order basis set[47] reduces the endergonities by approximately 1.0 kcal/mol, suggesting correlation error may be the cause, but it is not corrected adequately.

(47) (a) Chai, J. D.; Head-Gordon, M. Long-Range Corrected Hybrid Density Functionals with Damped Atom-Atom Dispersion Corrections. *Phys. Chem. Chem. Phys.* **2008**, *10*, 6615. (b) Dunning, T. H., Jr. Gaussian Basis Sets for Use in Correlated Molecular Calculations. I. The Atoms Boron Through Neon and Hydrogen. *J. Chem. Phys.* **1989**, *90*, 1007.

(48) For a NaHMDS/sodium enolate mixed aggregate characterized crystallographically, see ref 17e.

(49) Mixed solvates can show correlated solvation wherein the binding constant is markedly altered by the ligand on the distal metal of the dimer.[15]

(50) Although $^{29}Si-^{15}N$ coupling ($J_{Li\text{-}Si}$ = 8.8 Hz) confirms the dimer remains intact at all MTBE concentrations, $J_{N\text{-}Si}$ coupling is insensitive to whether ketone or MTBE is bound.

(51) Pocker, Y.; Buchholz, R. F. Electrostatic Catalysis by Ionic Aggregates. I. The Ionization and Dissociation of Trityl Chloride and Hydrogen Chloride in Lithium Perchlorate-Diethyl Ether Solutions. *J. Am. Chem. Soc.* **1970**, *92*, 2075.

(52) Tsoureas, N.; Mansikkamäki, A.; Layfield, R. A. Uranium(IV) Cyclobutadienyl Sandwich Compounds: Synthesis, Structure and Chemical Bonding. *Chem. Commun.* **2020**, *56*, 944.

(53) Bhattacharyya, D. N.; Lee, C. L.; Smid, J.; Szwarc, M. Studies of Ions and Ion Pairs in Tetrahydrofuran Solution. Alkali Metal Salts of Tetraphenylboride. *J. Phys. Chem.* **1965**, *69*, 608.

https://doi.org/10.1021/jacs.1c06529
J. Am. Chem. Soc. 2021, 143, 17452−17464

(54) For a particularly incisive comparison of the methods for calculating alkali metal solvation using both explicit and continuum models of solvation (including lithium and sodium solvated by THF and DME), see: Ziegler, M. J.; Madura, J. D. Solvation of Metal Cations in Non-aqueous Liquids. *J. Solution Chem.* **2011**, *40*, 1383.

(55) For additional computations of solvated sodium cation, see: (a) Lambert, C.; von Rague Schleyer, P. Are Polar Organometallic Compounds "Carbanions"? The Gegenion Effect on Structure and Energies of Alkali-Metal Compounds. *Angew. Chem., Int. Ed. Engl.* **1994**, *33*, 1129. (b) Chandrasekhar, J.; Jorgensen, W. L. The Nature of Dilute Solutions of Sodium Ion in Water, Methanol, and Tetrahydrofuran. *J. Chem. Phys.* **1982**, *77*, 5080. (c) Wu, Q.; Zaikowski, L.; Kaur, P.; Asaoka, S.; Gelfond, C.; Miller, J. R. Multiply Reduced Oligofluorenes: Their Nature and Pairing with THF-Solvated Sodium Ions. *J. Phys. Chem. C* **2016**, *120*, 16489.

(56) (a) $^{+}Na(\kappa^3\text{-PMDTA})_2$: Borys, A. M.; Hevia, E. Synthesis of a Stable Solvated Sodium Tris-Amido Nickelate. *Organometallics* **2021**, *40*, 442. (b) $^{+}Na(\kappa^2\text{-PMDTA})_2$: Graham, D. V.; Hevia, E.; Kennedy, A. R.; Mulvey, R. E.; O'Hara, C. T.; et al. Building an Extended Inverse Crown Motif *via* Alkali-Metal-Mediated α-Magnesiation of Furan. *Chem. Commun.* **2006**, 417.

(57) Collum, D. B. Is *N,N,N′,N′*-Tetramethylethylenediamine a Good Ligand for Lithium? *Acc. Chem. Res.* **1992**, *25*, 448.

(58) Wiedemann, S. H.; Ramírez, A.; Collum, D. B. Lithium 2,2,6,6-Tetramethylpiperidide-Mediated α- and β-Lithiations of Epoxides: Solvent-Dependent Mechanisms. *J. Am. Chem. Soc.* **2003**, *125*, 15893.

(59) There is an enormous number of documented $^{+}Na(THF)_6$ and $^{+}Na(\kappa^2\text{-DME})_3$ gegenions. For examples, see: (a) Livingstone, Z.; Hernan-Gomez, A.; Baillie, S. E.; Armstrong, D. R.; Carrella, L. M.; Clegg, W.; Harrington, R. W.; Kennedy, A. R.; Rentschler, E.; Hevia, E. Assessing the Reactivity of Sodium Alkyl-magnesiates Towards Quinoxaline: Single Electron Transfer (SET) vs. Nucleophilic Alkylation Processes. *J. Chem. Soc., Dalton Trans.* **2016**, *45*, 6175. (b) Also, see ref 56b.

(60) Reyes-Rodríguez, G. J.; Algera, R. F.; Collum, D. B. Cosolvent, and Isotope Effects on Competing Monomer- and Dimer-Based Pathways. *J. Am. Chem. Soc.* **2017**, *139*, 1233.

(61) Cram, D. J.; Gosser, L. Electrophilic Substitution at Saturated Carbon. XXI. Isoracemization Reactions Involving Ion-Pair Intermediates. *J. Am. Chem. Soc.* **1964**, *86*, 5457.

(62) Walborsky, H. M.; Youssef, A. A.; Motes, J. M. Cyclopropanes, XII. The Cyclopropyl Carbanion. *J. Am. Chem. Soc.* **1962**, *84*, 2465.

(63) Seebach, D.; Laube, T.; Dunitz, J. D. Über die Wechselwirkung zwischen Lithium-enolaten und sekundären Aminen in Lösung und im Kristall. *Helv. Chim. Acta* **1985**, *68*, 1373.

(64) Kawabata, T.; Fuji, K. Memory of Chirality: Asymmetric Induction Based on the Dynamic Chirality of Enolates. *Topics in Stereochemistry* **2003**, *23*, 175.

(65) Davis, F. A.; Zhang, Y.; Qiu, H. Asymmetric Synthesis of anti- and syn-2,3-Diamino Esters using Sulfinimines. Water and Concentration Effects. *Org. Lett.* **2007**, *9*, 833.

(66) $^{+}Li(THF)_6$: Schenk, C.; Henke, F.; Santiso-Quinones, G.; Krossing, I.; Schnepf, A. $[Si(SiMe_3)_3]_6Ge_{18}M$ (M = Cu, Ag, Au): Metalloid Cluster Compounds as Unusual Building Blocks for a Supramolecular Chemistry. *Dalton Trans.* **2008**, 4436.

(67) Wang, Y.; Song, S.; Xu, C.; Hu, N.; Molenda, J.; Lu, L. Development of Solid-State Electrolytes for Sodium-Ion Battery—A Short Review. *NMS* **2019**, *1*, 91.

(68) Kofron, W. G.; Baclawski, L. M. A Convenient Method for Estimation of Alkyllithium Concentrations. *J. Org. Chem.* **1976**, *41*, 1879.